Development of a temperature-programed electron-stimulated desorption ion angular distribution/time-of-flight system for real-time observation of surface processes and its application to adsorbed layers on Ru(001)

Takehiko Sasaki and Yasuhiro Iwasawa[a)]
Department of Chemistry, Graduate School of Science, The University of Tokyo, Hongo, Bunkyo-ku, Tokyo 113, Japan

(Received 10 February 1998; accepted for publication 21 July 1998)

A temperature-programed (TP) electron-stimulated desorption ion angular distribution (ESDIAD)/time-of-flight (TOF) system was developed in order to observe surface processes in real time by ESDIAD images and to measure TOF spectra of desorbing ions for identification of the mass and the kinetic-energy distribution of ions. The instrumentation of this system is described. This system was applied to $(\sqrt{3}\times\sqrt{3})R30°$-CO/Ru(001) (0.33 ML) and CO-saturated Ru(001) surfaces. As for the $(\sqrt{3}\times\sqrt{3})R30°$-CO/Ru(001), the increase of the half width at half maximum of the ESDIAD images upon annealing was found corresponding to the thermal excitation of the bending mode and/or hindered translation. On the other hand, as for the CO-saturated surface, the static disorder of the molecular axis of CO was larger, and apparent thermal excitation was not observed. After partial desorption of CO from the CO-saturated surface where the surface changes into the $\sqrt{3}\times\sqrt{3}$ structure at 400–430 K, the yield of O^+ increased due to the change in the adsorption site of CO. TOF spectra for ammonia adlayers (NH_3 and ND_3) were also measured by the developed system and the isotopic ratios for ESD yields depending on the adsorption states (chemisorbed first layer and physisorbed second layer) were obtained. © *1998 American Institute of Physics.* [S0034-6748(98)02610-0]

I. INTRODUCTION

Electron-stimulated desorption ion angular distribution (ESDIAD) has been demonstrated as a potential method to acquire information on the configuration of adsorbates on solid surfaces.[1] This technique has been used to obtain structural information of various adsorbates and reaction intermediates on solid surfaces. Many instruments and systems have been developed for measurements of ESD and ESDIAD. Yates and co-workers have developed a digital ESDIAD system and applied it to many chemisorption systems.[2] Mass-selected ESDIAD images by adopting a pulse-gated detection system has been realized by Madey and co-workers.[3,4] Recently Ahner *et al.* reported a time-of-flight (TOF) ESDIAD system acquiring a momentum-resolved ESDIAD image.[5] These systems require several seconds to 100 s to obtain an ESDIAD image. Though the images obtained by repeated anneal–quench procedures have been shown in many cases, to the best of our knowledge ESDIAD has not been used to monitor continuous chemical changes at active surfaces in real time. There might be two reasons for this limitation. One reason is a rather long acquisition time. The other relates to the temperature control of the sample. Surface chemical reactions occur usually at elevated temperatures or in temperature-programed conditions. Annealing of a sample is usually carried out by resistive heating, which induces a magnetic field near the sample, and hence, affects the motion of desorbing ions from the sample surface. These problems should be circumvented in order to utilize ESDIAD as a method for monitoring surface reactions in real time.

For the purpose of achieving this aim, we have developed an instrument which can measure ESDIAD images and TOF spectra of desorbing ions during the course of temperature-programed reactions and during chemical processes at constant temperatures. A pulsed incident electron beam and a pulsed heating current synchronized out-of-time phase with a repetition frequency of 12.8 kHz were adopted in this study. The whole system will be called the temperature-programed (TP)-ESDIAD/TOF system hereafter. Several studies on an electron-beam blanking technique for elevated temperatures have been published. Tracy reported a temperature controller for low-energy electron diffraction (LEED) at high temperature with the repetition frequency of 62.5 Hz.[6] Thomas and Weinberg reported a temperature controller for use of high-resolution electron-energy-loss spectroscopy (HREELS) measurement at elevated temperature at 0.3 Hz.[7] Riedl and Menzel measured ESDIAD of CO on Ru(001) at elevated temperature using a quadrupole mass spectrometer by rotating a sample, where alternatively chopped electron beam and electron bombardment for heating at 30 Hz were adopted.[8] In this study we also report a low-cost circuit for measuring TOF spectra with a repetition frequency of 2 kHz. It is noted that TOF measurements, which are used for identification of mass and translational energy distribution of desorbing ions, have been carried out by several groups.[9–17]

[a)]Corresponding author; electronic mail: iwasawa@chem.s.u-tokyo.ac.jp

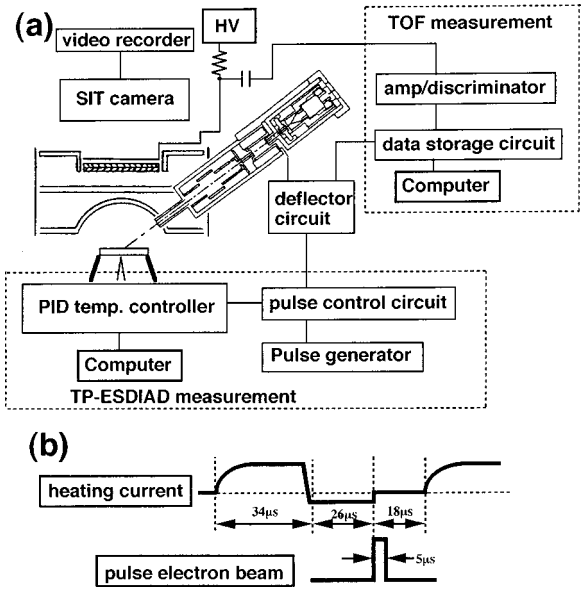

FIG. 1. (a) Schematic diagram for the TP-ESDIAD/TOF system. (b) Pulse sequences of electron beam and heating current for TP-ESDIAD measurements. The amplitude of heating current is modulated by a PID controller.

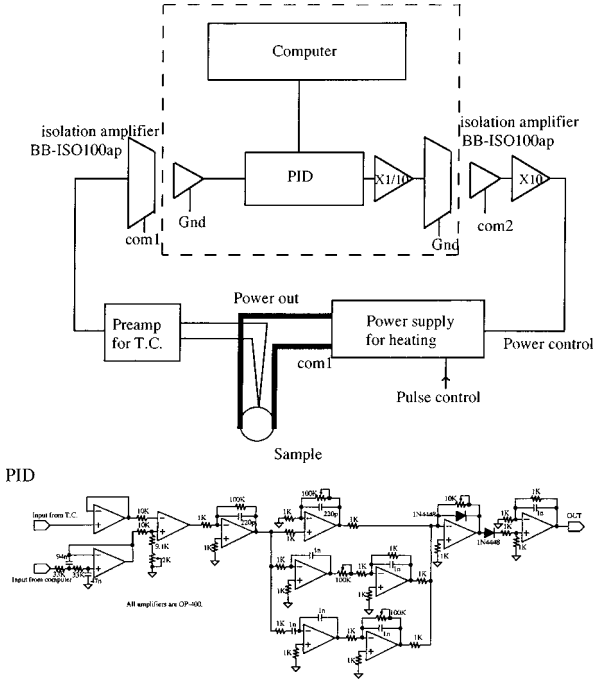

FIG. 2. Design for PID temperature controller under application of bias voltage to the sample.

In this article we report the instrumentation of a TP-ESDIAD/TOF system and its application to adsorption systems on Ru(001). The TP-ESDIAD/TOF system has already been used to observe coadsorption systems of ammonia and CO,[18] methylamine and CO,[19] and acetylene and CO on Ru(001),[20] and a decomposition process of methanol on Ru(001)-$p(2\times2)$-O.[21]

II. INSTRUMENTATION

The diagram of the TP-ESDIAD/TOF system is shown in Fig. 1(a). ESDIAD optics placed in an UHV chamber is comprised of a microchannel plate (MCP) with a phosphor screen, two plane grids, two hemispherical grids, and an electron gun which can emit a continuous electron beam and a pulsed one with a variable duration. The effective diameter of the MCP is 4 cm. The MCP, located 4 cm away from the sample surface, accepts desorbing ions within a polar angle of $\pm45°$ from the surface normal. There are three operating modes, (1) conventional ESDIAD measurement using a continuous electron beam, (2) temperature-programed ESDIAD measurement using a pulsed electron beam and a pulsed resistive heating current for the sample, and (3) TOF measurement of desorbing ions at a fixed (elevated) temperature. A silicon intensifier target (SIT) camera (C2741-8, Hamamatsu Photonics Co.) was used to record the ESDIAD images appearing on the phosphor screen on video tape. The incident angle of the electron beam is 55° from the surface normal. The primary energy of the electron beam can be set from 10 to 1000 eV. All measurements in the present study were performed with the primary electron energy of 350 eV, in which the sample current was 0.16 μA in the continuous mode. In the case of the temperature-programed ESDIAD, distortion of the trajectories of desorbing ions by a magnetic field induced by a heating current must be avoided. Therefore, a pulsed electron beam and a synchronized pulsed resistive heating current were adopted [Fig. 1(b)] so that the heating current remains zero during the flight of the pulsed electron beam and desorbing ions. The repetition frequency is 12.8 kHz and the duration of the electron beam is 5 μs. The sample current in the temperature-programed ESDIAD can be estimated to be 10.3 nA. Temperature control of the sample was performed by a proportional integral derivative (PID) controller. Bias voltage can be applied to the sample during temperature controlling as shown in Fig. 2. Two isolation amplifiers (Burr–Brown ISO-100AP) were adopted to read and control the temperature of the sample floating at a bias voltage with respect to the ground level. The PID circuit receives a reference voltage output from a computer corresponding to a programed temperature and compares it with a measured temperature, giving a signal (power control) to regulate the power supply for resistive heating. There are three common levels, Gnd, com1, and com2, where Gnd is the ground level, ''com1'' corresponds to the bias voltage with respect to the Gnd, and ''com2'' is higher by 5 V than ''com1'' for the use of pulsed resistive heating. Figure 3 shows the designs for the pulse control circuit, deflector circuit, and power supply for heating. The pulse control circuit creates two pulses for the incident electron pulse and pulsed resistive heating from a 12.8 kHz signal. The deflector circuit produces the pulse for electron-beam blanking at the deflector. The power supply for heating enables pulsed resistive heating with a voltage amplitude regulated by the PID circuit. The pulse control circuit generates trigger pulses for the electron beam and resistive heating by using single shot integrated circuit (74LS221) with an input pulse coming from a frequency-variable pulse generator. The phases of the pulses can be adjusted by changing the variable resistors associated with the 74LS221. When the deflector circuit, having a photocoupler (TLP554), accepts a transistor–transistor logic (TTL) pulse from the pulse control circuit, a negative

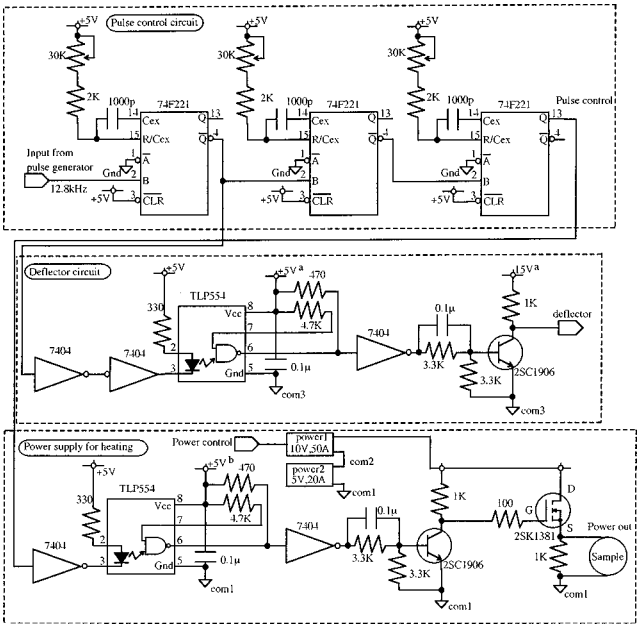

FIG. 3. Designs for pulse control circuit, deflector circuit, and power supply for heating.

pulse with an amplitude of 15 V is applied to the deflector, changing the voltage for the deflector from (15 V+com3) to com3, so that the electron beam is allowed to pass through the deflector electrodes. Pulsed resistive heating is performed by switching on and off the heating current using a metal–oxide–semiconductor field-effect transistor (2SK1381) with a control signal mediated by a photocoupler. Two power supplies were connected in series, a 5 V constant power supply with a capacity of 20 A and a voltage-variable power supply (10 V, 50 A) regulated externally by the power control (0–10 V) from the PID circuit. This connection means that the voltage amplitude varies from 5 to 15 V for stable temperature control.

The heating rate adopted in the present study was 0.5 K/s. An ESDIAD image corresponding to each temperature was acquired by summing 30 digitized video frames. This procedure implies that an image contains the contribution from the temperature range of 0.5 K. The ESDIAD images obtained using a pulsed electron beam do not look blinking because of the rather long lifetime (50–2000 μs) of phosphor (P-20). It is evident that this system is effective for measuring ESDIAD images during elevating temperature of the sample, whereas the distortion and broadening of the images are apparent when the sample is annealed by a continuous heating current during a conventional ESDIAD measurement. An ESDIAD image at 550 K was recorded as a background image due to emission of soft x ray and this component was subtracted from all images.[2]

TOF measurements were carried out using an incident electron beam with a duration of 150 ns. The arrival of electron pulses on the screen of the MCP is converted into a TTL pulse by an amplifier/discriminator (Hamamatsu Photonics Co. C3866). Pulse counting and accumulation were performed by a home-built data storage circuit with a time resolution of 10 ns controlled by a personal computer (NEC PC-9801 with Intel 486SL, 50 MHz). The repetition frequency was 2 kHz when a scanning time length was set to be 5.12 μs. In TOF measurements, after receiving a trigger pulse from the computer, a pulse is sent to a deflector of the electron gun, and the counter timers (74F191) are set to start. Signal pulses coming from the screen electrode of the MCP assembly are amplified and discriminated through the amplifier/discriminator and are sampled by four parallel D-Flip Flops (74F74) with four different phases, resulting in a sampling rate of 100 MHz. Sampled data are stored in a 128 kbytes static random access memory (SRAM) (HM62832, 8 bit X 32K, Hitachi Co.). Since data are latched by clocks with four phases, only 4 bits of each address are used and the other 4 bits are kept at low level. The connection between the data storage circuit and the computer is mediated by a conventional interface card assembled by us with 24 bits for output and 16 bits for input. After each scan, data in the memory are read by the computer to accumulate a TOF spectrum.

Figure 4 shows a design for the data storage circuit comprised from six blocks [Figs. 4(a)–4(f)]. (a) Formation of clocks. Four 25 MHz clock pulses (CLK1–CLK4) with a duty ratio of 1:3 and different phases are formed from a 100.0000 MHz quartz oscillator. Q2 is a 50 MHz signal with a 1:1 duty cycle, which is used to control the SRAM. $\overline{\text{CLRSIG}}$ is a clear pulse given by the computer. (b) Addressing for writing. Address for writing data on the SRAM is formed by four serial counters. A0–A15 are the address bus for the data storage circuit. A15 is not used for memory. A connection marked as an asterisk in Fig. 4 is chosen from a, b, and c to select a scanning time length of 5.12, 10.24, and 20.48 μs. A signal ''final'' is produced after the scanning time is over to initiate the memory reading procedure by the computer. (c) Addressing for reading. Address for reading data from the SRAM is given from the computer. Co0–Co15 are out-ports of the computer. (d) Timing for starting and finishing the pulse counting. Pulse counting (scanning) is initiated by the ''start pulse'' from the computer, yielding the ''$\overline{\text{RUN}}$'' signal that enables counting and the ''pulse out'' signal that is sent to the deflector circuit to send an incident electron pulse. After the ''final'' signal is received from (b) the ''interrupt'' signal will be sent to inform the computer of the end of one scanning. (e) Sampling. The input signal is sampled by four clocks (CLK1–CLK4). 4 bit data are latched by the 74F574 and delivered to the data bus (D0–D3) by the 74F541. D4–D7 are not used and always kept at the ground level. (f) Memory access. SRAM (HM62832) needs ''$\overline{\text{WE}}$'' (write enable), ''$\overline{\text{OE}}$'' (out enable), and ''$\overline{\text{CS}}$'' (chip select) signals for writing and reading data. Two 74F541 provide three signals appropriate for either writing or reading according to the signals ''$\overline{\text{WRITE}}$'' and ''$\overline{\text{READ}}$'' from the computer. Ci0–Ci7 are in-ports of the computer, exporting data to the computer.

The current of the electron beam during TOF measurements corresponded to 0.048 nA. TOF spectra in the present study were obtained after 10^5 repetitions, which corresponded to an acquisition time of about 1 min. In the case of TOF measurements integrating over the whole solid angle, heating was carried out not by a pulsed current but by a

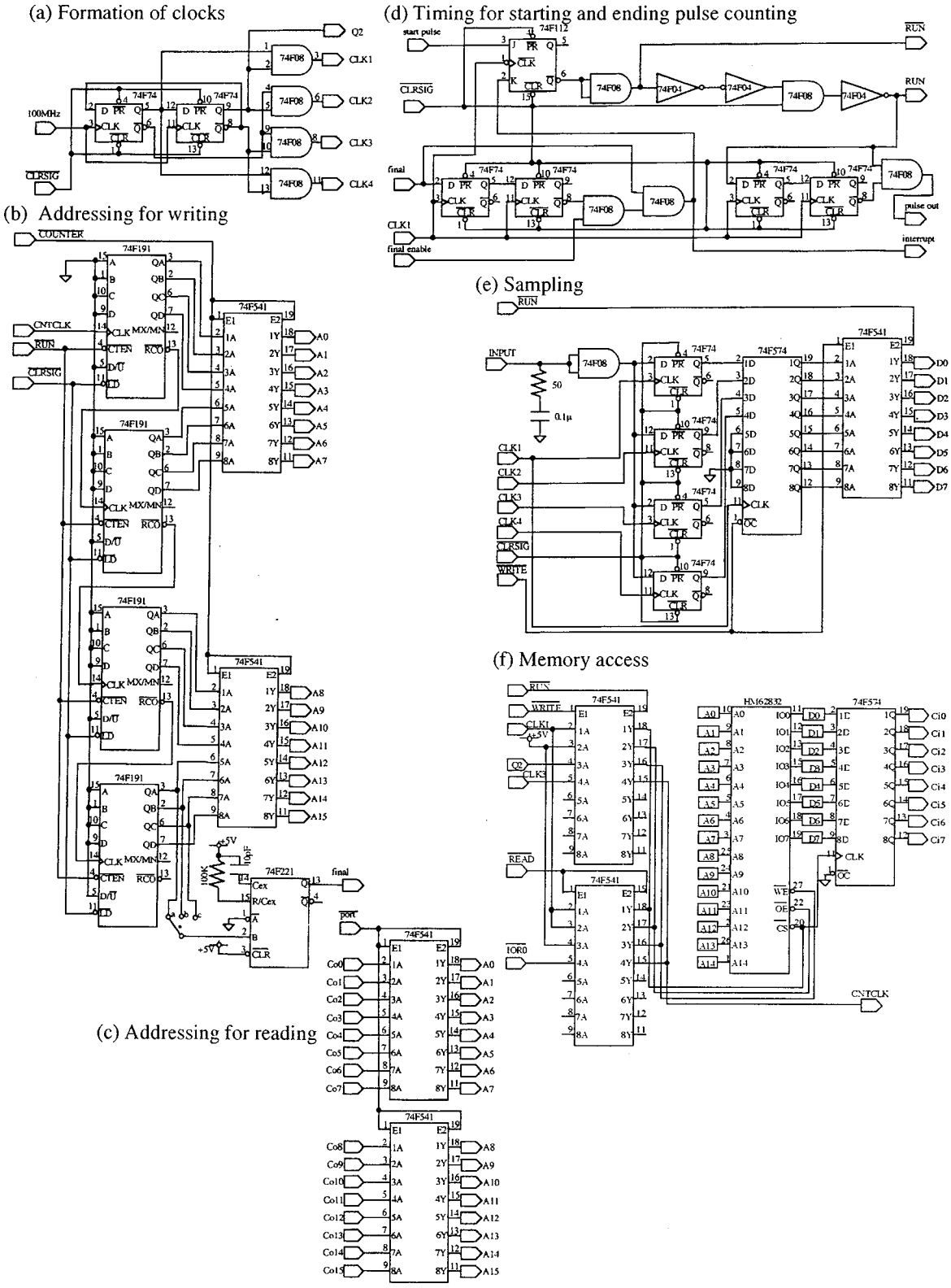

FIG. 4. Data storage circuit for TOF measurements of ESD ions with a time resolution of 10 ns, that is comprised of six blocks, (a) formation of clocks, (b) addressing for writing, (c) addressing for reading, (d) timing for starting and ending pulse counting, (e) sampling, and (f) memory access.

continuous one to minimize noise in the spectra.

Since the data storage circuit is driven by a 100 MHz clock, all parts were soldered on copper patterns fabricated by photoresist and etching on an epoxy resin board. A program for handling the data storage circuit was described with a C compiler.

III. TEMPERATURE-PROGRAMED ESDIAD MEASUREMENTS

The TP-ESDIAD/TOF system was used to monitor CO molecules adsorbed on Ru(001). Figure 5(a) shows an ESDIAD image and an intensity profile for $(\sqrt{3}\times\sqrt{3})R30°$-

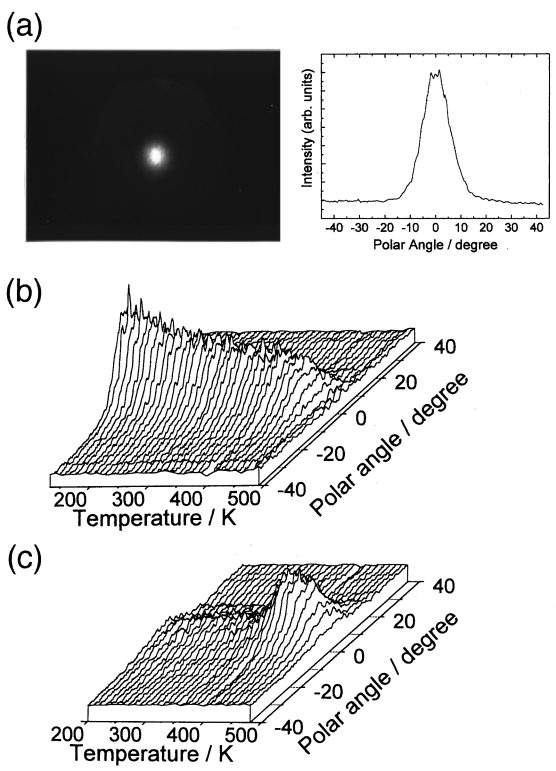

FIG. 5. (a): ESDIAD image and intensity profile for CO (0.33 ML) measured at 130 K. (b) and (c): Intensity profiles of TP-ESDIAD images versus temperature for $(\sqrt{3}\times\sqrt{3})R30°$-CO/Ru(001) (0.33 ML) and CO-saturated surface (0.68 ML), respectively.

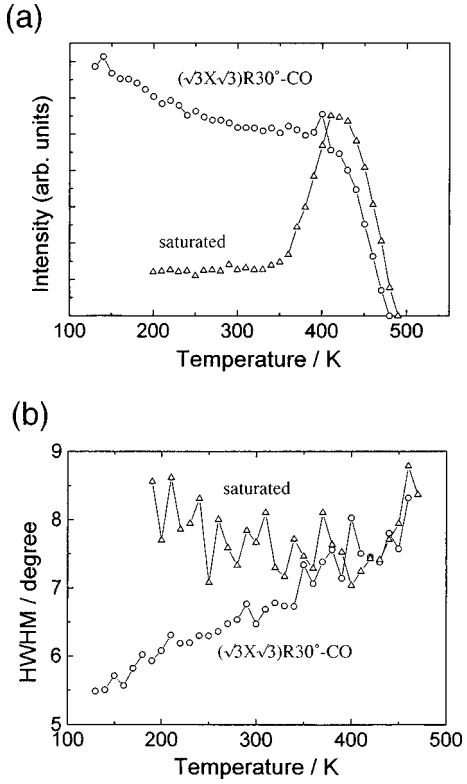

FIG. 6. Variations of intensity (a) and HWHM (b) with temperature for TP-ESDIAD images. Circles: $(\sqrt{3}\times\sqrt{3})R30°$-CO/Ru(001); triangles: CO-saturated surface.

CO/Ru(001) ($\theta_{CO}=0.33$ ML) at 130 K. The bias applied to the sample was 95 V. In this ESDIAD image the main desorbing ions are O^+ as evidenced by the TOF spectra shown below. The ESDIAD image is azimuthally symmetric with respect to the surface normal. The intensity profile was expressed in a Gaussian line shape with a half width at half maximum (HWHM) of 5.5°. This value of the HWHM represents the compressed one due to the bias voltage, and is in agreement with previous studies,[8,22] considering the bias voltage.

Figures 5(b) and 5(c) are the results of the temperature-programed ESDIAD for $(\sqrt{3}\times\sqrt{3})R30°$-CO/Ru(001) ($\theta_{CO}=0.33$ ML) and the CO-saturated Ru(001) ($\theta_{CO}=0.68$ ML), respectively, in the temperature range from 130 to 500 K. The ESDIAD images of the CO-saturated surface below 200 K are not shown in Fig. 5(c) because the contribution of H^+ due to adsorbed hydrogen originated from residual gas is larger than that of O^+ as found by TOF measurements. The images were obtained during annealing the sample at the rate of 0.5 K/s.

In Fig. 6 the intensity (a) and HWHM (b) of the ESDIAD images were plotted as a function of temperature. In the case of the $(\sqrt{3}\times\sqrt{3})R30°$-CO/Ru(001) the intensity monotonously decreased up to 400 K. After 400 K, at which desorption of CO started, the intensity decreased more steeply. As to the CO-saturated surface, the intensity was small and almost constant up to 350 K. The intensity started to increase rapidly after 350 K, where CO started to desorb and took a maximum at 400–430 K, corresponding to the $(\sqrt{3}\times\sqrt{3})R30°$ structure. At higher temperatures the intensity decreased in a similar way to the case of the $(\sqrt{3}\times\sqrt{3})R30°$ structure.

IV. TOF MEASUREMENTS

TOF measurements by the TP-ESDIAD/TOF system are shown in Fig. 7. Figure 7(a) is the TOF spectrum for the $(\sqrt{3}\times\sqrt{3})R30°$ structure at 100 K. A peak at 0 μs corresponds to the emission of the soft x ray stimulated by the incident electron pulses. Peaks of H^+, O^+, and CO^+ are observed at 0.31, 1.2, and 1.6 μs, respectively. The relative intensity ratio of O^+ to CO^+ is similar to the TOF spectrum for CO/Ni(110) measured by a TOF-ESD system.[23] Figure 7(b) shows TOF spectra for the CO saturated surface measured during stepwise annealing (20 K step below 340 K and 10 K steps above 360 K). The peak height intensities of O^+ and CO^+ versus temperature are plotted in Fig. 8 based on Fig. 7(b). It was found that the intensity of O^+ took a maximum at 400 K, corresponding to the ESDIAD images, while CO^+ did not show any maximum. It is clear that the coverage effect in the ESD cross section is specific for O^+. A possible reason for the negligible coverage effect for CO^+ may be either no enhancement effect for CO^+ or cancellation by neutralization at smaller coverages. The probability for neutralization of desorbing ions by electrons of the substrate may increase as the coverage decreases. The effect of neutralization on desorption of O^+ is less than that on CO^+ desorption,[8] which yields different profiles in the TOF spectra between O^+ and CO^+.

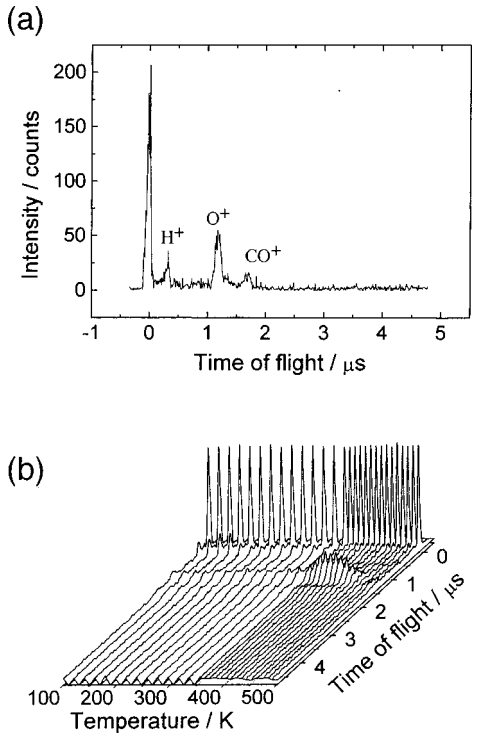

FIG. 7. (a) TOF spectrum measured for $(\sqrt{3}\times\sqrt{3})R30°$-CO/Ru(001) at 100 K. (b) TP-TOF spectra for the CO-saturated surface measured during the stepwise annealing in the temperature range from 100 to 500 K. A TOF spectrum was obtained after repetition of 10^5 incident electron pulses.

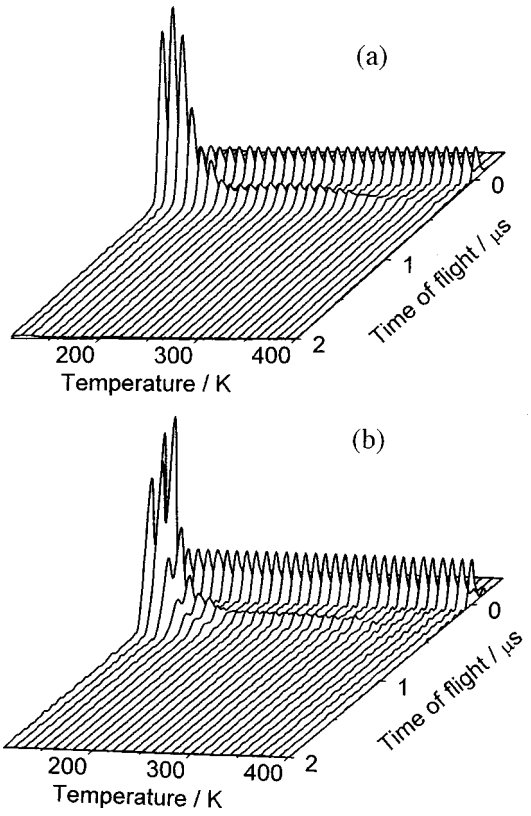

FIG. 9. TP-TOF spectra as a function of temperature for NH_3 (a) and ND_3 (b) on Ru(001). The surface was exposed to 2.0 L of NH_3 or ND_3 at 100 K.

TOF measurements were also carried out for the adsorption of NH_3 and ND_3 on Ru(001) in order to detect the difference in mass among isotopic species. Figures 9(a) and 9(b) show TOF spectra as a function of temperature for NH_3 and ND_3 on Ru(001), respectively, at an exposure of 2.0 L at 100 K. Figures 10(a) and 10(b) show the yields of H^+ and D^+ as a function of temperature based on Figs. 9(a) and 9(b), respectively. Peaks at 0.31 and 0.44 μs correspond to H^+ and D^+. The H^+ yield is very large below 130 K and decreases up to 180 K, reaching a plateau that vanishes at 350 K. These measurements showed that this system can discriminate H^+ and D^+ clearly. In ESDIAD measurements a strong and broad pattern centered along the surface normal for the second layer ammonia (0.5 ML) and a halo pattern for the monolayer ammonia (below 0.25 ML) were observed in agreement with published results.[24]

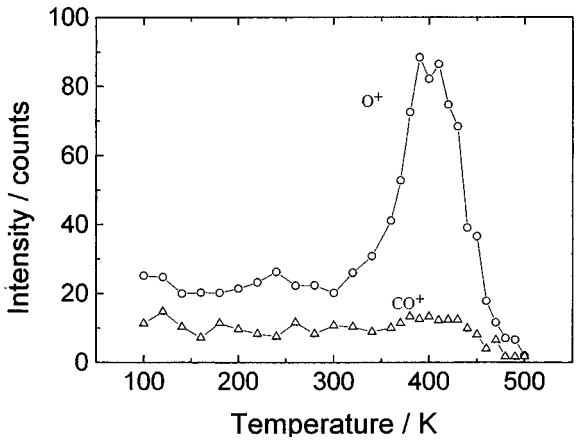

FIG. 8. Intensity of O^+ (circles) and CO^+ (triangles) versus temperature based on Fig. 7(b).

V. DISCUSSION

The TP-ESDIAD/TOF system developed in this study enables the measurement of continuous temperature-programed ESDIAD images in real time. This is an advantageous point in comparison with ESDIAD measurements after anneal–quench cycles. The present method can detect the change in adsorption layers as a fingerprint over a wide temperature range with a data acquisition time as short as that for temperature-programed desorption (TPD), while TPD detects desorption products upon annealing. The limitation of this system is the fact that a mass-resolved ESDIAD image cannot be taken. However, identification of desorbing ions is possible by independent TOF measurements, resulting in an appropriate interpretation of ESDIAD images. In this system real-time ESDIAD measurement has been given priority over mass-resolved measurement, which is expected to need a longer data acquisition time up to several minutes for one image. By using the TP-ESDIAD/TOF system aspects were found for well-studied adsorption layers, CO/Ru(001) and NH_3/Ru(001).

CO on Ru(001) has been investigated in detail not only by ESD and ESDIAD but also by other surface science techniques. CO molecularly adsorbs on Ru(001) with a saturation coverage of 0.68 ML.[25,26] The ordered structures of CO on Ru(001) are $(\sqrt{3}\times\sqrt{3})R30°$ at 0.33 ML, $(2\sqrt{3}\times2\sqrt{3})R30°$ at

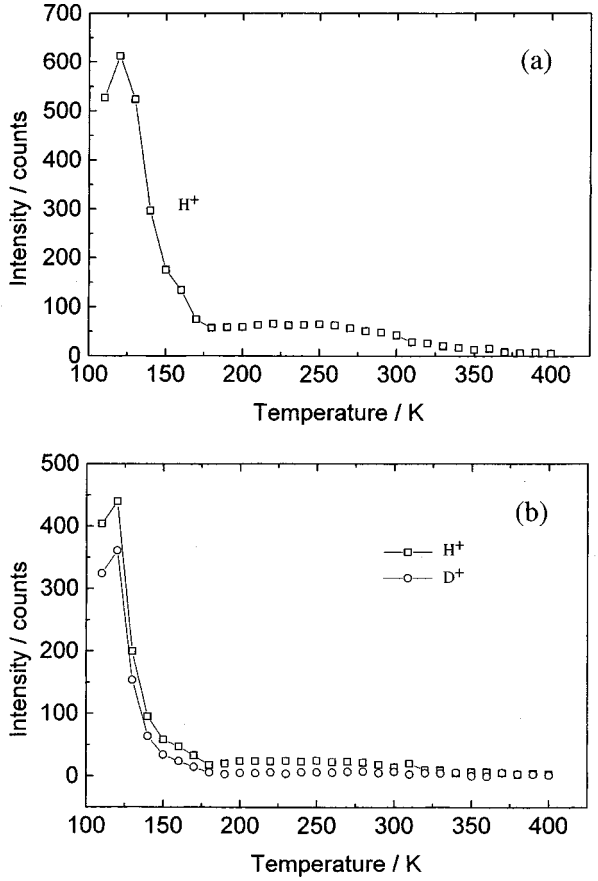

FIG. 10. (a) Yield of H^+ as a function of temperature based on Fig. 9(a). (b) Yields of H^+ and D^+ as a function of temperature based on Fig. 9(b).

0.58 ML, and a more compressed superstructure at the saturation coverage.[27] CO in the $(\sqrt{3}\times\sqrt{3})R30°$ structure is located at the top site as characterized by LEED I/V analysis.[28] Slight deviation from the top site as well as slight inclination of the C–O bond from the surface normal at the saturated coverage has also been proposed.[29] Recent LEED structural analysis revealed that experimental $I-V$ curves were simulated with improvement by assuming an anisotropic distribution of oxygen atoms in $(\sqrt{3}\times\sqrt{3})R30°$-CO/Ru(001) and that the molecular axis of the CO molecules is tilted on the average by $(12\pm3)°$ at 150 K.[30] The temperature dependence of the carbon and oxygen mean-square deviations was found to be consistent with the bending mode of the CO molecule with excitation energy of 5 ± 1 meV.[31] In the TPD spectrum for the CO-saturated Ru(001) surface there are two CO desorption peaks at 410 K (α_1) and at 470 K (α_2).[25,26] After the α_1 desorption the surface changes into the $(\sqrt{3}\times\sqrt{3})R30°$ structure and the α_2-desorption peak originates from CO adsorbed on the top sites. Madey measured ESD measurements for O^+ and CO^+ including temperature dependence.[22] Dependence of the primary energy on the yield of desorbed ions from CO/Ru(001) was studied by Feulner *et al.*[32] Riedl and Menzel reinvestigated the angular distribution of O^+ and CO^+ using a quadrupole mass spectrometer and suggested that CO is inclined on the average by 5° to the normal in the saturated layer.[33] They also studied the influences of surface temperature below 250 K, coverage, and primary energy of incident electrons.[8] The coverage (exposure) dependence of the ESD intensity for CO/Ru(001) was reported by Madey[22] who showed that the intensity of desorbing O^+ ions took the maximum at the exposure to CO corresponding to the $(\sqrt{3}\times\sqrt{3})R30°$ structure. This dependency was interpreted as the change in the bonding of CO (e.g., out of registry displacements due to lateral interactions). Riedl and Menzel also suggested that the coverage effect on the ESD intensity was caused by the change in the binding energy and/or site changes as well as some possible steric hindrance by neighbors.[8] The result in Fig. 6 can be understood in a similar way. The adsorption site for CO is the top site in the case of the $(\sqrt{3}\times\sqrt{3})R30°$ structure and at higher coverages there is a small displacement from the top site as well as inclination of the molecular axis,[29] leading to the change in the electronic state of adsorbed CO, and hence, yielding the change in the ESD cross section.

The temperature dependence of the HWHM [Fig. 6(b)] differs with the CO coverage. The HWHM for the $(\sqrt{3}\times\sqrt{3})R30°$ structure increased from 5.5° to 8.5° almost linearly upon annealing, corresponding to the thermal excitation of the hindered translation and bending motion.[22] On the other hand, the HWHM for the CO-saturated surface remained constant at about 7.5° up to 400 K and increased a little above 400 K. Tilt of the CO axis from the surface normal has been suggested by several groups,[8,22,29,33] resulting in a large HWHM at low temperatures. The constant HWHM during annealing in Fig. 6(b) may be caused by the restriction of thermal excitation due to the short distance between CO [3.28 Å for the saturated surface, which is shorter than 4.69 Å in the $(\sqrt{3}\times\sqrt{3})R30°$ structure], or thermal excitation may not be outstanding because of the large static disorder in the saturated surface.

The extent of damage in the surface adlayer caused by electron beams during the measurements should be mentioned here. The time necessary for temperature-programed ESDIAD from 100 to 520 K is 14 min and that for whole TOF measurements from 100 to 520 K with a step of 10 K is 45 min. The damage in the CO-saturated layer by the electron beam during the data acquisition time was estimated. The cross sections for O^+ and CO^+ desorption have been reported to be $1-5\times10^{-18}$ cm^2.[33] Here, assuming that the cross section of electron-stimulated processes for the CO-saturated surface is 5×10^{-18} cm^2, and that the width of the electron beam is 1 mm^2, the damages in the adsorption layer were estimated to be 2.7% for temperature-programed ESDIAD and 0.04% for the TOF measurements, indicating the negligible effect of the electron beam. This small extent of damage indicates that observed changes are due to thermal processes.

Adsorption of ammonia on Ru(001) is another example which has been studied in detail by TPD,[34] ESDIAD,[24] and HREELS.[35] The temperature-dependent change shown in Figs. 10(a) and 10(b) corresponds to the change in adsorption layer, i.e., multilayer, second layer, and monolayer ammonia.[35] The neutralization process for desorbing ions, which reduces the ESD ion yield, is less significant for thicker layers. Chemisorbed ammonia persists on the surface up to 350 K.[35]

In the case of ND_3, not only D^+ but also H^+ appears with a comparable intensity. These H^+ ions resulted from the partial isotopic exchange that took place on a $B-A$ gauge or through a variable leak valve during exposure to ND_3. It is possible to estimate the isotopic ratio of the ESD yield $[y(H^+)/y(D^+)]$ and the ratio of the H–D exchange (H/D mixing ratio) by comparing Figs. 10(a) and 10(b). As to the second layer ammonia (150 K), the $y(H^+)/y(D^+)$ is 3.5 and the H/D mixing ratio is 33%. As to the monolayer ammonia (200 K) the $y(H^+)/y(D^+)$ is 7.0 and the H/D mixing ratio is 41%. The H/D mixing ratio with a similar extent was observed as the coexistence of ν(N–H) and ν(N–D) in HREELS spectra of ND_3 by our group.[36] The ratio of the ESD yield $[y(H^+)/y(D^+)]$ showed a marked difference between the second layer and the first layer. The nearer the bond to be disrupted approaches the surface, the larger the $y(H^+)/y(D^+)$ becomes, indicating that the heavier ion (D^+) is more easily neutralized near the surface than the lighter ion (H^+), probably due to the slower motion. The isotopic ratio of the ESD yield has not been associated with the distance from the surface so far, but the present result suggests that their correlation should be analyzed theoretically.

In summary, a TP-ESDIAD/TOF system was developed to monitor surface processes in real time. This system can measure temperature-programed ESDIAD images and TOF spectra of desorbing ions in addition to conventional ESDIAD images. The CO/Ru(001) surfaces during the temperature-programed desorption processes were monitored by this system. Temperature-dependent changes in the ESDIAD images were observed. TOF spectra for ammonia adlayers (NH_3 and ND_3) were also measured and the isotopic ratios for ESD yields depending on the adsorption state (chemisorbed layer and second layer) were estimated.

ACKNOWLEDGMENT

This work has been supported by CREST (Core Research for Evolutional Science and Technology) of the Japan Science and Technology Corporation (JST).

[1] R. D. Ramsier and J. T. Yates, Jr., Surf. Sci. Rep. **12**, 243 (1991).
[2] M. J. Dresser, M. D. Alvey, and J. T. Yates, Jr., Surf. Sci. **169**, 91 (1986).
[3] S. A. Joyce, A. L. Johnson, and T. E. Madey, J. Vac. Sci. Technol. A **7**, 2221 (1989).
[4] N. J. Sack, L. Nair, and T. E. Madey, Surf. Sci. **310**, 63 (1994).
[5] J. Ahner, D. Mocuta, R. D. Ramsier, and J. T. Yates, Jr., J. Vac. Sci. Technol. A **15**, 1548 (1997).
[6] J. C. Tracy, Rev. Sci. Instrum. **39**, 1300 (1968).
[7] G. E. Thomas and W. H. Weinberg, J. Vac. Sci. Technol. **16**, 87 (1979).
[8] W. Riedl and D. Menzel, Surf. Sci. **207**, 494 (1989).
[9] R. Stockbauer, E. Bertel, and T. E. Madey, J. Chem. Phys. **76**, 5639 (1982).
[10] N. D. Shinn and T. E. Madey, Surf. Sci. **180**, 615 (1987).
[11] K. Ueda and A. Takano, Jpn. J. Appl. Phys., Part 2 **27**, L2029 (1988).
[12] K. Ueda and A. Takano, Jpn. J. Appl. Phys., Part 1 **28**, 2594 (1989).
[13] I. Arakawa, M. Takahashi, and K. Takeuchi, J. Vac. Sci. Technol. A **7**, 2090 (1989).
[14] S. L. Bennett, C. L. Greenwood, and E. M. Williams, Surf. Sci. **290**, 267 (1993).
[15] H. Daimon, Rev. Sci. Instrum. **59**, 545 (1988).
[16] H. Daimon and S. Ino, Vacuum **41**, 215 (1990).
[17] K. Sakamoto, K. Nakatsuji, H. Daimon, T. Yonezawa, and S. Suga, Surf. Sci. **306**, 93 (1994).
[18] T. Sasaki and Y. Iwasawa, Surf. Sci. Lett. **384**, L798 (1997).
[19] T. Sasaki, Y. Itai, and Y. Iwasawa, Surf. Sci. **390**, 17 (1997).
[20] T. Sasaki, Y. Itai, and Y. Iwasawa, J. Electron. Spectrosc. Relat. Phenom. **88-91**, 773 (1998).
[21] T. Sasaki, Y. Itai, and Y. Iwasawa, Chem. Lett. 1125 (1997).
[22] T. E. Madey, Surf. Sci. **79**, 575 (1979).
[23] A. Takano and K. Ueda, Jpn. J. Appl. Phys., Part 1 **30**, 1847 (1991).
[24] C. Benndorf and T. E. Madey, Surf. Sci. **135**, 164 (1983).
[25] H. Pfnür and D. Menzel, J. Chem. Phys. **79**, 2400 (1983).
[26] H. Pfnür, P. Feulner, and D. Menzel, J. Chem. Phys. **79**, 4613 (1983).
[27] E. D. Williams and W. H. Weinberg, Surf. Sci. **82**, 93 (1979).
[28] G. Michalk, W. Moritz, H. Pfnür, and D. Menzel, Surf. Sci. **129**, 92 (1983).
[29] G. E. Thomas and W. H. Weinberg, J. Chem. Phys. **70**, 1437 (1979).
[30] H. Over, W. Moritz, and G. Ertl, Phys. Rev. Lett. **70**, 315 (1993).
[31] M. Gierer, H. Bludau, H. Over, and G. Ertl, Surf. Sci. **346**, 64 (1996).
[32] P. Feulner, R. Treichler, and D. Menzel, Phys. Rev. B **24**, 7427 (1981).
[33] W. Riedl and D. Menzel, Surf. Sci. **163**, 39 (1985).
[34] L. R. Danielson, M. J. Dresser, E. E. Donaldson, and J. T. Dickinson, Surf. Sci. **71**, 599 (1978).
[35] J. E. Parmeter, Y. Wang, C. B. Mullins, and W. H. Weinberg, J. Chem. Phys. **88**, 5225 (1988).
[36] T. Sasaki, T. Aruga, and Y. Iwasawa, Surf. Sci. **240**, 223 (1990).